

Interacting anyonic fermions in a two-body color code model

H. Bombin,¹ M. Kargarian,² and M. A. Martin-Delgado³

¹*Department of Physics, Massachusetts Institute of Technology, Cambridge, Massachusetts 02139, USA*

²*Department of Physics, Sharif University of Technology, Tehran 11155-9161, Iran*

³*Departamento de Física Teórica I, Universidad Complutense, 28040 Madrid, Spain*

(Received 28 April 2009; published 13 August 2009)

We introduce a two-body quantum Hamiltonian model of spin $\frac{1}{2}$ on a two-dimensional spatial lattice with exact topological degeneracy in all coupling regimes. There exists a gapped phase in which the low-energy sector reproduces an effective color code model. High-energy excitations fall into three families of anyonic fermions that turn out to be strongly interacting. The model exhibits a $\mathbf{Z}_2 \times \mathbf{Z}_2$ gauge-group symmetry and string-net integrals of motion, which are related to the existence of topological charges that are invisible to moving high-energy fermions.

DOI: [10.1103/PhysRevB.80.075111](https://doi.org/10.1103/PhysRevB.80.075111)

PACS number(s): 75.10.Jm, 03.65.Vf, 05.30.Pr, 71.10.Pm

I. INTRODUCTION

The Kitaev model on the honeycomb lattice¹ has attracted a great deal of attention in the recent years^{2–5} since it offers the opportunity to study many properties of topologically ordered systems in a very well-suited scenario for condensed matter. One of the most interesting properties of the Kitaev model is that one of its phases effectively reproduces the famous toric code. This is the first example of topological quantum error correction and plays a major role in quantum information.

Yet, there is another family of topological codes, color codes, which exhibit very remarkable properties. They allow an appropriate implementation of the whole Clifford group of quantum gates, which are essential in quantum information tasks.⁶ Topological color codes (TCC) are constructed with quantum lattice Hamiltonians that typically demand six-body terms in a two-dimensional (2D) spatial lattice, requirements quite unrealistic in a condensed-matter framework. Up to now, it has remained a challenge to find a two-body Hamiltonian capable of hosting a TCC in a particular coupling regime.

In this paper we provide such a two-body spin- $\frac{1}{2}$ Hamiltonian model. It turns out to exhibit very rich physics and, quite remarkably, it does not belong to the family of models originated after Kitaev's model. These latter models are defined on trivalent lattices, which allows a fermionization yielding a free fermion exact solution. Instead, the lattice of our model is 4 valent, a sharp difference that prevents complete solvability and gives rise to very interesting features not present in the mentioned models: (i) exact topological degeneracy in all coupling regimes, rooted on the existence of string-net integrals of motion. This degeneracy, related to certain “invisible” topological charges, is 4^g fold in surfaces of genus g . (ii) emergence of three families of strongly interacting fermions with semionic relative statistics. (iii) an exact $\mathbf{Z}_2 \times \mathbf{Z}_2$ gauge symmetry. Each family of emergent fermions sees a different \mathbf{Z}_2 gauge subgroup.

Thus, the model admits an exact analysis of many interesting properties. This is so mainly because there exist local integrals of motion in an amount of $\frac{1}{3}$ of the total number of spins.

Although we will focus on a particular phase of the model, namely, the one that effectively yields TCCs, a rich phase diagram beyond this gapped phase is to be expected in analogy with.¹ This includes the possibility of non-Abelian anyons and other phases with interesting many-body effects. In addition, it is possible to break a symmetry of the model, which we call color symmetry whereas the exact features above are kept. This paves the way to a yet more complex phase diagram.

The properties of the model make it a good candidate for an experimental realization, by means of some engineering scheme such as polar molecules on optical lattices.⁷ It is also amenable to numerical computations⁸ with several methods, which would help to uncover some of its nonperturbative aspects and phases.

In summary, the model represents a relevant contribution to the difficult task of searching for systems with emerging anyons and topological order, which are conceptually important phenomena and a source of physics.

This paper is organized as follows: in Sec. II we introduce the quantum Hamiltonian model based solely on two-body interactions between spin- $\frac{1}{2}$ particles. The lattice is two dimensional and has coordination number 4, instead of the usual 3 for the Kitaev model. It is pictured in Fig. 1 and it is called ruby lattice. In Sec. III, we introduce a mapping from the original spin- $\frac{1}{2}$ degrees of freedom onto bosonic degrees of freedom in the form of hard-core bosons which also carry a pseudospin. In Sec. IV, we describe the constants of motion of our model, specifying both its various types (normal strings and nonstandard stringnets), as well as its number of $\frac{1}{3}$ of the total number of spins. With the help of the previous mapping, it is possible to analyze very interesting qualitative features of our model at nonperturbative level. In Sec. V, we show how the emerging quasiparticle excitations of our model are anyonic fermions with strong interactions, which are a manifestation of the string-net structure of the constants of motion. Thus, the model is not a free fermion model. In Sec. VI, we solve the problem of finding a two-body quantum lattice Hamiltonian hosting the topological color code as one of its phases. Interestingly enough, the relevant properties of the TCC remain valid at the nonperturbative level as well. We also describe the notion of invisible charges and

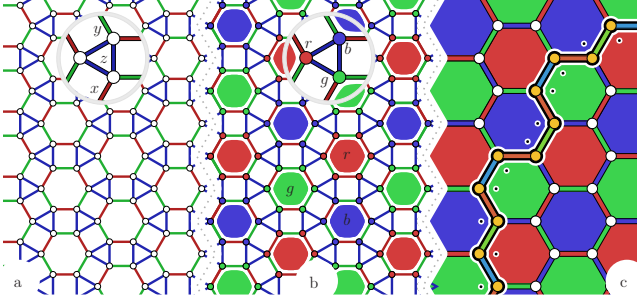


FIG. 1. (Color online) Three different points of view of the system. In (a,b) blue links form triangles and red and green links form hexagons. (a) is the physical one, with vertices representing spins and colored links representing $\sigma_a^x \sigma_b^x$, $\sigma_a^y \sigma_b^y$, and $\sigma_a^z \sigma_b^z$ two-body interactions. In (b) both spins and hexagonal plaquettes have been colored. (c) is the reduced lattice Λ , where vertices represent sites, that is, the blue triangles of (a). We show a magnified site in [(a) and (b)] and a closed string in (c).

discuss anyon condensation, and its implications. Section VII is devoted to conclusions.

II. HAMILTONIAN MODEL WITH TWO-BODY INTERACTIONS

The model of interest lives in the lattice of Fig. 1(a). Notice that, unlike in Refs. 1–4, it has coordination 4. Vertices represent spin- $\frac{1}{2}$ systems and links two-body interactions. The Hamiltonian is

$$H = - \sum_{\langle i,j \rangle} J_w \sigma_i^w \sigma_j^w, \quad w = \begin{cases} x, & \text{red links} \\ y, & \text{green links} \\ z, & \text{blue links} \end{cases}, \quad (1)$$

where the couplings $J_w \neq 0$ are real, σ^w are the Pauli matrices and the sum extends over all links. Notice that blue links are special since they form triangles, which we will refer to as *sites* for reasons that will be apparent below.

Sites are the vertices of a reduced lattice Λ in which links are given by the pairs of parallel red and green links of the original lattice, see Fig. 1(c). This reduced lattice will play an essential role in the study of the properties of the model. It is an hexagonal lattice and thus has 3-colorable plaquettes. We choose to color them with red (r), green (g), and blue (b). We also color links accordingly, in such a way that c links connect c plaquettes. Here and in what follows, we use the letter c to denote color variables. We remark that this coloring has nothing to do with the one used for links in Fig. 1(a). The coloring of the reduced lattice induces a coloring of some plaquettes of the original lattice, see Fig. 1(b), and also a vertex coloring that labels the spins within a site.

Although we have given a particular lattice for concreteness, the analysis that follows is much more general. Instead of having a hexagonal reduced lattice, it could be any trivalent lattice with 3-colorable plaquettes. Such lattices were named 2-colexes in Ref. 9. Any closed surface will work, orientable or not. That the construction works on nonorientable surface is a consequence of the equivalence of vertex bicolorability and orientability in 2-colexes.¹⁰

III. BOSONIC MAPPING

In Sec. VI we will analyze in detail the regime $J_z > 0$, $|J_x|, |J_y| \ll J_z$. Let us set for simplicity $J_z = 1/4$. Then in the extreme case $J_x = J_y = 0$ the system consists of isolated triangles, one per site. In an energy eigenstate, each of them contributes an energy $-3/4$ or $1/4$ so that we can attach a quasiparticle with energy gap equal to 1 to each triangle. With this motivation, we give here a map to a system in which these quasiparticles are explicit. The mapping is *exact* so that only the physical picture is changed. It has the advantage of isolating those degrees of freedom that survive once the integrals of motion to be described below have been fixed.

In Fig. 1(b) each spin in a site has been identified with a color. We label the corresponding Pauli operators as σ_c^w with $c = r, g, b$. Consider the Hilbert space \mathcal{H}_C with orthonormal basis $\{|0\rangle, |r\rangle, |g\rangle, |b\rangle\}$ and introduce the colored annihilation operators

$$b_c := |0\rangle\langle c|, \quad c = r, g, b, \quad (2)$$

so that \mathcal{H}_C represents a hard-core boson with three possible color states. The number operator n and the colored number operator n_c are

$$n := \sum_c n_c, \quad n_c := b_c^\dagger b_c. \quad (3)$$

At each site, we attach such a boson and also an effective spin $\frac{1}{2}$. We have to relate this degrees of freedom to the original three spins in the site, which are colored as in Fig. 1(b). The mapping can be expressed by relating bases of both systems. In particular, taking the usual up/down basis for the three physical spins and the tensor product basis

$$|a, d\rangle = |a\rangle \otimes |d\rangle, \quad a = \uparrow, \downarrow, \quad d = 0, r, g, b, \quad (4)$$

for the effective spin and hard-core boson system we have

$$|\uparrow, 0\rangle \equiv |\uparrow\uparrow\uparrow\rangle, \quad |\downarrow, 0\rangle \equiv |\downarrow\downarrow\downarrow\rangle, \quad (5)$$

$$|\uparrow, r\rangle \equiv |\uparrow\downarrow\downarrow\rangle, \quad |\downarrow, r\rangle \equiv |\downarrow\uparrow\uparrow\rangle, \quad (6)$$

$$|\uparrow, g\rangle \equiv |\downarrow\uparrow\downarrow\rangle, \quad |\downarrow, g\rangle \equiv |\uparrow\downarrow\uparrow\rangle, \quad (7)$$

$$|\uparrow, b\rangle \equiv |\downarrow\downarrow\uparrow\rangle, \quad |\downarrow, b\rangle \equiv |\uparrow\uparrow\downarrow\rangle. \quad (8)$$

More compactly, the mapping can be expressed by identifying operators as follows:

$$\sigma_c^z \equiv \tau^z \otimes p_c, \quad \sigma_c^v \equiv \tau^v \otimes (b_c^\dagger + b_c + s_v r_c), \quad (9)$$

where $v = x, y$, $s_x := -s_y := 1$, the symbols τ denote the Pauli operators on the effective spin and we are using the color parity operators p_c and the color switching operators r_c defined as

$$p_c := 1 - 2(n_{\bar{c}} + n_{\bar{\bar{c}}}), \quad r_c := b_{\bar{c}}^\dagger b_{\bar{\bar{c}}} + b_{\bar{\bar{c}}}^\dagger b_{\bar{c}}, \quad (10)$$

where the bar operator transforms colors cyclically as follows:

$$\bar{r} := g, \quad \bar{g} := b, \quad \bar{b} := r. \quad (11)$$

From this point on we will be working always in the reduced lattice Λ . For compactness, we will use a simplified notation in which site indices are suppressed and only relative positions are indicated; the notation $O_{,c}$ means O applied at the site, that is, connected to a site of reference by a c link. For example, if i, j, k are neighboring sites, with i the reference site and j, k are connected to i by a g link and a r link, respectively, then instead of $A_i B_j C_k$ we write $AB_{,g}C_{,r}$. That is, we only indicate the relationship between sites and completely omit the reference site i , which is therefore implicit. Also, we indicate the $w=x, y, z$ indices of J_w , τ^w , and s_w in terms of two colors as follows:

$$c|c := z, \quad \bar{c}|c := x, \quad \bar{\bar{c}}|c := y. \quad (12)$$

Then, the Hamiltonian (1) can be exactly transformed into a new form

$$H = -3N/4 + Q - \sum_{\Lambda} \sum_{c \neq c'} J_{c'|c} T_c^{c'}, \quad (13)$$

with N the number of sites, $Q := \sum_{\Lambda} n$ the total number of hard-core bosons, the first sum running over the N sites of the reduced lattice, the second sum running over the six combinations of different colors c, c' and

$$T_c^{c'} = u_c^{c'} + \frac{t_c^{c'} + v_c^{c'}}{2} + \frac{r_c^{c'}}{4} + \text{H.c.}, \quad (14)$$

a sum of several terms for an implicit reference site, according to the notation convention we are using. The meaning of the different terms in Eq. (14) is the following. The operator $t_c^{c'}$ is a c -boson hopping, $r_c^{c'}$ switches the color of two \bar{c} or $\bar{\bar{c}}$ bosons, $u_c^{c'}$ fuses a c boson with a \bar{c} boson (or a $\bar{\bar{c}}$ boson) to give a \bar{c} boson (\bar{c} boson) and $v_c^{c'}$ destroys a pair of c bosons. A pictorial representation is offered in Fig. 2(a). The explicit expressions are

$$t_c^{c'} := \tau_c^{c'} b_c b_{c,c'}^{\dagger}, \quad r_c^{c'} := \tau_c^{c'} r_c r_{c,c'}, \quad (15)$$

$$u_c^{c'} := s_{c'|c} \tau_c^{c'} b_c r_{c,c'}, \quad v_c^{c'} := \tau_c^{c'} b_c b_{c,c'}, \quad (16)$$

where we are using the notation

$$\tau_c^{c'} := \tau^{c'|c} \tau_{c,c'}^{c'}. \quad (17)$$

IV. CONSTANTS OF MOTION

In this section we explore several integrals of motion of the Hamiltonian (13).

A. Color charge

A basic property of the Hamiltonian (13) is the existence of a $\mathbf{Z}_2 \times \mathbf{Z}_2$ charge. Let us label the elements of $\mathbf{Z}_2 \times \mathbf{Z}_2$ with colors as $\{e, r, g, b\}$, where e is the identity element. We also label its irreps as $\{\chi_e, \chi_r, \chi_g, \chi_b\}$ setting $\chi_e(c) := \chi_c(c) := -\chi_c(\bar{c}) = 1$. Let us arbitrarily attach a charge to each family

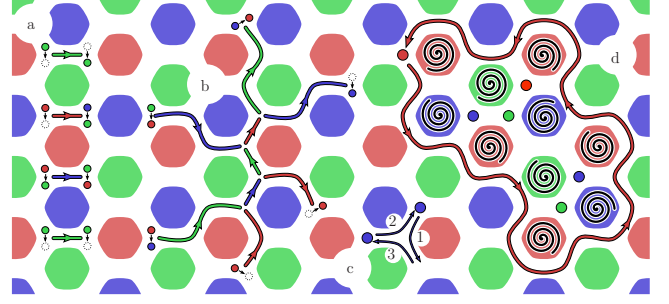


FIG. 2. (Color online) Several c -fermion processes, in the effective hexagonal lattice. c fermions are depicted as c -colored balls and their movement with c -colored directed strings. When the initial and final color charge at a site are different before and after a process, we show the transition with a small black arrow. (a) Examples of the effects of the terms in Eq. (13). From top to bottom, the corresponding terms are t_g^r , u_r^b , r_b^g , and v_g^r . (b) A typical c -fermion interaction process, with hoppings, fusions, and splittings. (c) The exchange of two identical b fermions. (d) An r fermion surrounds a region λ . The phase that it picks up depends both on the number of g and b fermions in λ and the vortex states of the plaquettes marked with an spiral.

of hard-core bosons. In particular, we attach the irrep χ_c to each c boson. Let $Q_c = \sum_{\Lambda} n_c$ be the total number of c bosons. The total color charge

$$\chi_{\Lambda} := \chi_r^{Q_r} \chi_g^{Q_g} \chi_b^{Q_b} \quad (18)$$

is preserved by the Hamiltonian. This can be checked directly or noting that the operators

$$\chi_{\Lambda}(c) = (-1)^{Q_c + Q_{\bar{c}}} = \prod_{\Lambda} p_c \quad (19)$$

commute with all the terms in Eq. (14). In Sec. V the meaning of color charge will become clear when we relate it to a $\mathbf{Z}_2 \times \mathbf{Z}_2$ gauge field.

B. Plaquette operators

We describe now certain plaquette operators that commute with each other and with each of the terms of the Hamiltonian. As we will show below, the corresponding degrees of freedom should be regarded as vortices. For each color c and each plaquette π there is a constant of motion of the form

$$S_{\pi}^c := \prod_{\pi} \tau^{c'|c} p_{c' \star c}, \quad (20)$$

where c' is the color of the plaquette π , the product runs through its sites, and \star is just a convenient symmetric color operator defined by

$$c \star c := c, \quad c \star \bar{c} := \bar{c} \star c := \bar{c}. \quad (21)$$

These operators are not all independent. They are subject only to the following constraints

$$\prod_{\pi \in \Lambda} S_{\pi}^c = (-1)^{N/2}, \quad \prod_{c=r,g,b} S_{\pi}^c = (-1)^{s/2}, \quad (22)$$

where s is the number of sites of a given plaquette π and we are supposing in the first equation that the lattice forms a closed surface. It follows that there are $2F-2$ independent plaquette operators, with F the number of faces, or plaquettes, of the reduced lattice Λ . The total color charge is not independent of plaquette operators because

$$\chi_{\Lambda}(c) = \prod_{\pi \in \Lambda_{\bar{c}}} S_{\pi}^{\bar{c}} \prod_{\pi \in \Lambda_{\bar{c}}} S_{\pi}^{\bar{c}}, \quad (23)$$

where Λ_c denotes the subset of c plaquettes of Λ .

In Sec. V we show that plaquette degrees of freedom can be regarded as vortices, as they correspond to a $\mathbf{Z}_2 \times \mathbf{Z}_2$ gauge field, which has therefore no dynamics. The correspondence between plaquette-operator eigenstates and group values is as follows. First, for each c plaquette we introduce the following alternative plaquette operators:

$$\begin{aligned} B_{\pi}^{\bar{c}} &:= j_x^{s/2} S_{\pi}^{\bar{c}}, \\ B_{\pi}^{\bar{c}} &:= j_y^{s/2} S_{\pi}^{\bar{c}}, \\ B_{\pi}^c &:= (-j_x j_y)^{s/2} S_{\pi}^c, \end{aligned} \quad (24)$$

where $j_w := J_w / |J_w|$. The element $g_{\pi} \in \mathbf{Z}_2 \times \mathbf{Z}_2$ that we attach to each plaquette π is determined, for a given eigenstate of the operators Eq. (24), by the conditions

$$\chi_c(g_{\pi}) = B_{\pi}^c. \quad (25)$$

These equations always have a solution because $(B_{\pi}^c)^2 = B_{\pi}^r B_{\pi}^g B_{\pi}^b = 1$. Given a region or collection of plaquettes λ , we will use the notation $g_{\lambda} := \prod_{\pi \in \lambda} g_{\pi}$.

C. String operators

Plaquette constants of motion can be generalized to closed strings and, for that matter, also to string nets.¹⁰ For a closed string we mean a connected path in the lattice with no end points, see Fig. 1(c). To any such string γ and color c we attach a string operator

$$S_{\gamma}^c := \prod_{\gamma} \tau^{c|c'} p_{c \star c'}, \quad (26)$$

where the product runs through the sites of γ and, for each site, c' is the color of the plaquette around which γ turns at the site. This is exemplified in Fig. 1(c), where we have marked with a dot the corresponding plaquette for each vertex of the string. As in the case of plaquette operators, we have $(S_{\gamma}^c)^2 = (-1)^{\frac{s}{2}} S_{\gamma}^c S_{\gamma}^{\bar{c}} = 1$ with s the number of sites of γ . Closed string operators commute with all plaquette operators and Hamiltonian terms but not always with each other. Namely, if the strings γ and γ' cross once then $[S_{\gamma}^c, S_{\gamma'}^c] = 0$ but $\{S_{\gamma}^c, S_{\gamma'}^{\bar{c}}\} = 0$.

This anticommutation property, which remarkably is not present in Ref. 1, turns out to be crucial. In systems with nontrivial topology it is the source of an exact degeneracy of

the Hamiltonian. For example, the lattices of Fig. 1 with periodic boundary conditions live on a torus, which has two independent nontrivial loops γ, γ' . Then S_{γ}^c anticommutes with $S_{\gamma'}^{\bar{c}}$ and commutes with $S_{\gamma}^{\bar{c}}$ and $S_{\gamma'}^c$, showing¹¹ that the Hamiltonian is at least fourfold degenerate. More generally, in a closed surface with Euler characteristic χ the degeneracy is $2^{2-\chi}$. In particular, in orientable surfaces of genus g there exist a 4^g -fold topological degeneracy. This result is exact and independent of the particular phase of the system we are in. In order to label the global flux degrees of freedom attached to nontrivial string operators we can use the eigenvalues of $2-\chi$ topologically nontrivial and independent closed string operators of a given color.

V. ANYONIC FERMIONS

In the previous section we have learned that the system is divided into sectors with a given vortex and global flux configuration. We now want to understand the nature of the degrees of freedom in each of these sectors and we start counting them. In terms of spin- $\frac{1}{2}$ degrees of freedom, the original system has $3N$ spins, the plaquette operators remove $2F-2$ of them and the nontrivial string operators of a given color $2-\chi$ more. These leaves $N' = 2N - \chi$ effective spins in a given sector. Since we are not interested in global degrees of freedom, let us suppose that the topology is trivial so that $2-\chi=0$. Then the resulting value of N' can be easily understood; we are only left with hard-core boson degrees of freedom (hence the $2N$), subject to the constraint of color charge preservation (hence the -2). In fact, in each sector we can choose a basis with elements labeled by the state of the hard-core bosons so that these become the relevant degrees of freedom. As we will see, the dynamics of the system transform the hard-core bosons into three families of fermions with anyonic statistics between them. Moreover, we will see that these fermions interact strongly. For arbitrary couplings this only provides us with a picture to understand the system since the emergent quasiparticles could be very different. However, in the regime analyzed in Sec. VI the anyonic fermions come to life explicitly.

In order to check the statistics of the effective quasiparticles emerging from hard-core boson degrees of freedom it suffices¹² to study the hopping terms in Eq. (13). Strictly speaking, the situation here is not the same as in Ref. 12 as we are not studying quasiparticles. More close is the approach in Ref. 1, where the emphasis is done on the properties of string operators. Now, we first note that the hopping terms $t_c^{\bar{c}}$ and $t_c^{\bar{c}}$ that appear in Eq. (13) are only enough to hop a c boson around a c plaquette. We need also composite hoppings: $t_c^c = u_{\bar{c}}^c u_{\bar{c},c}^{c\dagger} = u_{\bar{c}}^c u_{\bar{c},c}^{c\dagger}$ hops a c boson from a c plaquette to another. Notice that this notation completely agrees with Eq. (15). Consider a state with only two c -boson excitations, located at two sites separated, respectively, by a \bar{c} and a \bar{c} link from a given reference site, as in Fig. 2(c). We may then consider a hopping process, indicated with numbers in the figure, in which the c bosons are exchanged in such a way that local contributions cancel.¹ The net effect of exchanging the c bosons is

$$\bar{t}_{c,c}^{\bar{c}} t_{c,c}^{\bar{c}} \bar{t}_{c,c}^{\bar{c}} t_{c,c}^{\bar{c}} = (\tau^y \tau_{\bar{c}}^y \tau_{\bar{c}}^z \tau_{\bar{c}}^z \tau_{\bar{c}}^x \tau_{\bar{c}}^x)^2 = -1, \quad (27)$$

showing that the hard-core bosons give rise to fermions.¹²

These fermions carry a nontrivial color charge and thus we have three families of them. They are not free but interacting, as follows from the existence of the $u_c^{\bar{c}}$ terms in the Hamiltonian, which correspond to a 3-fermion interaction vertex, see Fig. 2(b). In fact, the existence of this vertex indicates that we are not dealing just with fermions but rather with anyons; three conventional fermions cannot fuse into the vacuum. In addition, fermions must be coupled to a non-trivial gauge field.¹²

In order to understand these two issues, let us consider a process in which a c fermion is carried around a region λ , as in Fig. 2(d). For clarity, we assume that no fermions but that to be transported are present along the boundary of λ . The hopping process yields a phase

$$\phi_\lambda^c = \chi_c(g_\lambda) (-1)^{n_c^\lambda + n_{\bar{c}}^\lambda + n_4^\lambda}, \quad (28)$$

where n_c^λ denotes the number of c fermions inside λ and n_4^λ the number of 2-colex plaquettes inside λ with a number of edges that is a multiple of four. We conclude that each family of fermions carries a different representation of a $\mathbf{Z}_2 \times \mathbf{Z}_2$ gauge group with values g_λ dictated by the vortex states. In addition, fermions of different color have semionic mutual statistics; they pick a-1 phase when one of them winds around the other. Thus, fermions not only interact via virtual fermion exchanges but also topologically.

VI. EFFECTIVE TOPOLOGICAL COLOR CODE

We now turn to a perturbative study of the regime $J_z > 0$, $|J_x|, |J_y| \ll J_z$, for which the previous bosonic mapping is specially suited. As in Ref. 13 we apply the PCUTs method¹⁴ (perturbative continuous unitary transformations). This method produces an effective Hamiltonian H_{eff} , at a given perturbation order such that $[H_{\text{eff}}, Q] = 0$. We are specially interested in the low-energy physics, that is, the $Q=0$ sector of the Hamiltonian (notice that the sectors here have nothing to do with the ones discussed in the previous section). For each c plaquette π let us set $B_\pi^x := B_\pi^{\bar{c}}$ and $B_\pi^y := B_\pi^{\bar{c}}$. Then since $Q=0$ we have

$$B_\pi^x = j_x^{s/2} \prod_{\pi} \tau^x, \quad B_\pi^y = j_y^{s/2} \prod_{\pi} \tau^y. \quad (29)$$

For the particular lattice of Fig. 1, the ninth order perturbative calculation yields, up to a constant, the effective Hamiltonian

$$H_{\text{eff}} = - \sum_{\pi \in \Lambda} (k_x B_\pi^x + k_y B_\pi^y + k_z B_\pi^x B_\pi^y), \quad (30)$$

with

$$k_z = \frac{3}{8} |J_x J_y|^3 + O(J^7), \quad (31)$$

$$\frac{k_x}{|J_y|^3} = \frac{k_y}{|J_x|^3} = \frac{55489}{13824} |J_x J_y|^3. \quad (32)$$

The Hamiltonian (30) describes a color code model on the effective spins.⁶ Its ground state is the vortex free sector, where $\chi_c(g_\pi) = 1$ for any plaquette π . Excitations are vortices, gapped, and localized at plaquettes with $B_\pi^x = -1$ and/or $B_\pi^y = -1$. At higher orders in perturbation theory the terms of the effective Hamiltonian take the form of products of vortex operators, which gives rise to vortex interactions.^{10,13}

Color code models have a topological order described by a $\mathbf{Z}_2 \times \mathbf{Z}_2$ quantum double.¹⁵ Thus there exist 16 topological charges in the model, labeled with pairs (g, χ) with $g \in \mathbf{Z}_2 \times \mathbf{Z}_2$ and χ an irrep of this group. The trivial charge or vacuum sector is (e, χ_e) , the charges (c, χ_c) , (e, χ_e) , and (c, χ_c) are bosons and $(c, \chi_{\bar{c}})$ and $(c, \chi_{\bar{c}})$ are fermions. As for the mutual statistics, moving a (g, χ) charge around a (g', χ') charge gives a topological phase $\chi(g') \chi'(g)$. Regarding fusion rules, a (g, χ) charge and a (g', χ') charge form together a $(gg', \chi\chi')$ charge. Notice how the three fermions $(c, \chi_{\bar{c}})$ form a family closed under fusion. The same is true for the three $(c, \chi_{\bar{c}})$ fermions. Two fermions from different families have no topological interaction. This property will turn out to be important in the understanding of the model.

There are several possible ways to label the excitations of the gapped phase Eq. (30). Our choice is that an excitation at a c plaquette π has (c, χ_e) charge if $-B_\pi^x = B_\pi^y = 1$, (e, χ_c) charge if $B_\pi^x = -B_\pi^y = 1$, and (c, χ_c) charge if $B_\pi^x = B_\pi^y = -1$.

A. Beyond the low-energy sector

We now turn our attention to the high-energy quasiparticles, that is, those which contribute to the quasiparticle counter Q . From the analysis of Sec. V we now that these are three families of interacting anyonic fermions. The virtual processes of these fermions create the gap for low-energy excitations, as well as interactions between them.

High-energy quasiparticles belong to a particular topological charge superselection sector. This correspondence between low- and high-energy excitations follows from the global constraints Eqs. (22) and (23), which have local consequences. Namely, the local creation of a single c fermion must be accompanied by the change in sign of several vortex operators, with the net result of the creation/annihilation of a low-energy $(\bar{c}, \chi_{\bar{c}})$ charge. This topological charge has exactly the properties needed to agree with the fermion fusion rules and the results (27) and (28) derived before.

Let us now take a closer look to the sector with $Q=1$, which involves no interactions. Using the PCUTs method one can derive the effective Hamiltonian for the gapped phase in the sector with a single c fermion, for a given color c . At first order the c fermion just hops around c plaquettes so that for $J=J_x=J_y$ we get a $-2J$ contribution to the energy gap coming from this orbital motion. Going to second order we get a nonflat dispersion relation that corresponds to the triangular lattice formed by c plaquettes. The gap, at this order, is given by $1 - 2J - J^2/2$ and thus it closes at $J \approx 0.45$. This is just an approximate estimation since we are omitting

all fermion interactions and, perhaps more importantly, we are taking $J \simeq J_z$. However, it is to be expected that as the couplings $J_x \sim J_y$ grow in magnitude the gap for high-energy fermions will reduce, producing a phase transition when the gap closes. Such a phase transition resembles the anyon condensations discussed in Refs. 16 and 17. Here we are dealing with a condensation of three anyonic fermions that does not fit those examples but part of the physical picture could be similar. There exist three nontrivial topological charges that do not interact with the three condensed anyons. We would thus expect a residual topological order in the new phase, with three nontrivial topological charges with relative semionic statistics. These charges would then be responsible for the 4^s exact topological degeneracy. This conjecture is to some extent supported by the validity in all phases of closed string integrals of motion which, as we will see next, represent processes related to the three topological charges invisible to the moving fermions.

B. Invisible topological charges

It is natural to expect that open c -string operators will create, transport, and destroy a particular topological charge among the 16 possible ones. But since string operators commute with the hopping terms in Eq. (13), the corresponding three charges must have bosonic relative statistic with respect to the moving high-energy fermions. That is, they must be “invisible” for them. This is indeed the case, since, as can be easily checked, c strings move $(\bar{c}, \chi_{\bar{c}})$ charges. These are three fermionic charges with semionic mutual statistics.

Such an invisibility feature for several charges with nontrivial mutual statistics is not present in the Kitaev model and has a potential qualitative advantage from an experimental perspective. In this regard, in Ref. 5 it was discussed how the high-energy fermions of the honeycomb model can spoil attempts to demonstrate the topological order. The fact that in the present model there exist topological charges invisible to high-energy fermions could simplify the operations needed to show the appearance of topological phases because a process that only involves the invisible charges is nothing but a product of string constants of motion.

VII. CONCLUSIONS AND PROSPECTS

We have presented a quantum lattice Hamiltonian in 2D spatial dimensions that models many relevant and interesting features regarding systems with quantum topological proper-

ties. An instance of this is the existence of string-nets configurations which are constants of motion of the Hamiltonian and are related to fermionic processes. This is a nonperturbative result, thus valid for any regime of coupling constants in the model.

Another prominent result is the emergence of fermionic quasiparticles with nontrivial relative statistic, that is, anyonic fermions. These fermions are not free but highly interacting, which makes difficult an analytical approach.

The model we have introduced deserves further study in many directions that we have motivated throughout our work and they are beyond the scope of this paper. We can mention hereby several prospects for future work.

The Hamiltonian (1) has the symmetries of the lattice in Fig. 1(a). We could consider a more general Hamiltonian, in such a way that some of these symmetries are lost and we are left only with those of Fig. 1(b). This amounts to explicitly break the color symmetry of the model by substituting the three couplings J_w with nine couplings J_w^c . The couplings J_z^c correspond to the blue bonds that connect a \bar{c} and a \bar{c} vertex, and the couplings J_x^c and J_y^c correspond, respectively, to the red and green bonds lying on c plaquettes, see Fig. 1(b). This gives rise to a richer phase diagram and physics. For example, in the effective color code phase the differences among the J_z^c couplings amounts to different gaps for r , g , and b fermions. Then different phase transitions will produce as each of the gap closes.

We have made a clear connection of the model with the topological color code, which appears as a gapped phase. We have found perturbative indications for the existence of other phases. Thus, it is desirable to continue the study of the whole phase diagram of the model using other types of techniques, including numerical simulations.

Another aspect that deserves further study is the properties of these models for quantum computation in a more explicit way since here we have only focused on their properties as far as topological order is concerned and its connections with topological color codes.

ACKNOWLEDGMENTS

We thank X.-G. Wen and J. Vidal for useful discussions and correspondence, respectively. We acknowledge financial support from a PFI under Grant No. EJ-GV, DGS grants under Contract No. FIS2006-04885 and the ESF under Contract No. INSTANS 2005-10.

¹A. Kitaev, Ann. Phys. **321**, 2 (2006).

²X.-Y. Feng, G.-M. Zhang, and T. Xiang, Phys. Rev. Lett. **98**, 087204 (2007).

³H. Yao and S. A. Kivelson, Phys. Rev. Lett. **99**, 247203 (2007).

⁴S. Yang, D. L. Zhou, and C. P. Sun, Phys. Rev. B **76**, 180404(R) (2007).

⁵S. Dusuel, K. P. Schmidt, and J. Vidal, Phys. Rev. Lett. **100**, 177204 (2008).

⁶H. Bombin and M. A. Martin-Delgado, Phys. Rev. Lett. **97**, 180501 (2006).

⁷A. Micheli, G. K. Brennen, and P. Zoller, Nat. Phys. **2**, 341 (2006).

⁸V. Lahtinen, G. Kells, A. Carollo, T. Stitt, J. Vala, and J. K. Pachos, Ann. Phys. **323**, 2286 (2008).

⁹H. Bombin and M. A. Martin-Delgado, Phys. Rev. B **75**, 075103 (2007).

- ¹⁰M. Kargarian, H. Bombin, and M. A. Martin-Delgado (unpublished).
- ¹¹M. Oshikawa and T. Senthil, Phys. Rev. Lett. **96**, 060601 (2006).
- ¹²M. Levin and X.-G. Wen, Phys. Rev. B **67**, 245316 (2003).
- ¹³J. Vidal, K. P. Schmidt, and S. Dusuel, Phys. Rev. B **78**, 245121 (2008).
- ¹⁴C. Knetter and G. Uhrig, Eur. Phys. J. B **13**, 209 (2000).
- ¹⁵F. A. Bais, Peter van Driel, and Mark de Wild Propitius, Phys. Lett. B **280**, 63 (1992).
- ¹⁶H. Bombin and M. A. Martin-Delgado, Phys. Rev. B **78**, 115421 (2008).
- ¹⁷F. A. Bais and J. K. Slingerland, arXiv:0808.0627 (unpublished).